Marine Chemistry
February 2008, Volume 109, Issues 1-2, Pages 98-114
http://dx.doi.org/10.1016/j.marchem.2007.12.007

Role of tidal pumping on nutrient cycling in a temperate lagoon (Arcachon Bay, France)

Jonathan Deborde[a, *], Pierre Anschutz[a], Isabelle Auby[b], Corine Glé[a], Marc-Vincent Commarieu[a], Daniele Maurer[b], Pascal Lecroart[a] and Gwenaël Abril[a]

[a]Université de Bordeaux I, CNRS, UMR 5805 Environnements Paléoenvironnements OCéaniques (EPOC), avenue des facultés, 33405 Talence, France
[b]Laboratoire IFREMER DEL/AR, Quai du Commandant Silhouette, 33120 Arcachon, France

*: Corresponding author : J. Deborde, email address : j.deborde@epoc.u-bordeaux1.fr

Abstract:

The hypothesis of nutrient-rich pore-waters seeping at low tide through sediments to channel waters, which drain tidal flats during ebb, was evaluated in the Arcachon lagoon. The back of the bay is affected by freshwater inputs and underground freshwater discharges. The upper part of tidal flat consists of permeable sandy sediments, which are covered by a muddy sediment layer on the lower part. Permeable sediments outcrop in the bed of channel web. Surface water chemistry and early diagenesis processes in sediment were estimated by collecting channel web waters and cores on a tidal flat and in channels at different seasons and time scales. Waters from tidal creeks are under-oxygenated, and enriched in reduced solutes. Muddy sediments showed evidences of strong organic matter mineralization and bioturbation. Underlying permeable sandy sediments revealed as well evidences of an enrichment of inorganic nutrients, and dilution with fresh continental groundwater. During ebb, tidal creek waters stem from mudflats by seeping of anoxic pore-waters, and from permeable sediments by advection of reduced waters. A rough estimation shows that the yearly contribution of this tidal pump of pore-waters for dissolved inorganic phosphorus (DIP) and ammonia inputs is of the same order of magnitude than river inputs for the studied part of the bay. Extrapolated to the whole Arcachon lagoon, pore-water discharge at low tide supplies to water column at least 556 kmol yr^{-1} and 18300 kmol yr^{-1} of DIP and NH_4^+, respectively. Tidal drainage at low tide represents therefore a minimal contribution of recycled nutrient of 55% for DIP and 15% for dissolved inorganic nitrogen to the lagoon.

Keywords: Tidal pump; Tidal creek water; Organic matter mineralization; Phosphorus; Nitrogen; Pore-waters seeping; Arcachon Bay

1. Introduction

Lagoon environments are highly dynamic systems controlled by physical processes and subjected to marine and continental influences. They play a key role as spawning grounds for fish and shellfish, and have been extensively exploited for aquaculture, fishing, tourism … Eutrophication is a naturally occurring process in most lagoons because of their function as a sink for nutrient inputs from land and sea (De Wit et al., 2001). Thus, processes controlling nutrient levels and distributions in lagoon environments must be understood to assess the impact of human activities and global natural change on the chemical cycling and ecology of these coastal ecosystems.

In lagoon ecosystems, where depth is low and intertidal zone is extended, the sediment becomes the central unit of biogeochemical nutrient cycles and intense biological productivity. During immersion, numerous studies demonstrated complex interactions and high exchanges between sediment and overlying water occurring in tidal environments (Falcao and Vale, 1995; Rocha et al., 1995; Rocha, 1998; Morin and Morse, 1999; Mortimer et al., 1999; Welsh et al., 2000; Sakamaki et al., 2006). The coupling between benthic processes and exchanges with water is linked to benthic production and deposition of organic matter, subsequent remineralization of organic matter with release of inorganic nutrients to pore-waters, and transport of dissolved nutrients back into overlying water column (Jahnke et al., 2003; Sakamaki et al., 2006). Thus, sediments are either sinks or sources of nutrients derived from external inputs and internal recycling processes. Early diagenesis products are transported to the water column through several processes. In addition to spontaneous molecular diffusion at the sediment water interface, transport of solute by bioturbation (irrigation from burrows and biodiffusion) and discharge of advective groundwater or seawater from bottom permeable sediment layers take place (Simmons, 1992; Huettel et al., 1998; Moore, 1999; Koretsky et al., 2002; Charette et al., 2005; Grigg et al., 2005; Meysman et al., 2006). During ebb, a large channel web drains intertidal flats. Sediment-channel water exchanges can be an important pathway for nutrient cycles and budget for lagoons (Agosta, 1985).

The present study focuses on the chemical composition of tidal creek waters that drain intertidal mudflats during ebb in a mesotidal coastal lagoon. We observed first that most of these creeks were not connected to surface flowing continental waters. Second, at low tide, and before flood tide reached the creeks, the runoff of flowing waters could not be explained by surface water eluviation. These observations suggested that waters flowing in tidal creeks originated partly from nutrient-rich pore-waters. Our objective was to verify this hypothesis, and to estimate the impact of these waters on the global nutrient cycle of the lagoon. Tidal creek waters were compared to samples collected in a channel connected to a river and to waters collected at high tide and during tide cycles. The connection between tidal creek waters and pore-water was evaluated by studying early diagenesis products in sediment cores collected on the tidal flat and in permeable channel sediment.

2. Study site, materials and methods

2.1. Arcachon Bay

Arcachon Bay is a mesotidal shallow lagoon of 180 km² located on the French Atlantic coast (44°40′ N, 1°10′ W; Fig. 1). It is a major centre for oyster farming, and recreational activities. It is connected to the Atlantic Ocean by a 2-3 km wide and about 12 km long channel, that enables important seawater exchanges, estimated at up to 384 x 10^6 m^3 for each tidal cycle (Plus et al., 2006). The tide is semi-diurnal and the tidal amplitude ranges from 1.1 m to 4.9 m (Gassiat, 1989). At low tide, in the inner lagoon (156 km^2), tidal channels drain large tidal flats (115 km²). The maximum water depth of main channels is 20 m. About 70 km^2 of tidal flats are covered by *Zostera noltii* meadows (Auby and Labourg, 1996; Blanchet et al., 2005). At high tide, surface water temperature fluctuates annually between 1 and 30°C, and surface water salinity between 22 and 32. The intertidal area is exposed to atmosphere for several hours, over each semi-diurnal tidal period. The back of the bay is affected by moderate river inputs and underground freshwater discharges, with a major part coming from the Leyre River, the remaining is provided by secondary streams (Rimmelin et al., 1998). The lower part of the intertidal zone consists of muddy sediments (grain size: 15 - 40 µm), and some upper parts are constituted with permeable sandy sediments (grain size: ~250 µm). Permeable sandy sediments also outcrop in the bed of the largest channels.

2.2 Study site

The studied site consists of a mud flat exposed to the atmosphere 12h per day at minimum. About 20% of the surface area is covered by macrophyte meadows (*Zostera noltii* and *Spartina anglica*). The upper part of the tidal flat is covered by more permeable sandy sediments. The study site is cut at southern side by a main channel connected to a small river, which annual mean discharge ranges from 0.120 to 0.160 $m^3\ s^{-1}$ (Fig. 2). The channel represents a small-scale estuary with a salinity gradient from 0 (in the small river) to 15 – 27, depending on season. Subsequently, we named this channel the estuarine channel. This channel is also the effluent of a web of tidal creeks (called regionally "*estey*"), which are not connected to surface continental water flows (Fig. 2). These creeks drain the mud flat at low tide. In the studied area, the main tidal creek was at low tide 400 m in length, between 0.5 and 3 m large, with a mean depth of 20 cm. Permeable sandy sediments outcrop in the bed of main branches of creeks and constitute a potential exchange area with underground water. Some portions of the sandy bed were red coloured, suggesting that sand grains were coated with iron oxides. The tidal creek water discharge was measured using a current-meter at several low tide periods, and was between 100 and 120 $l\ s^{-1}$ depending on phreatic level (wet-dry season) and tide (neap-spring). At low tide, upper parts of muddy intertidal flat present 1 to 10 m large and about 10 cm deep tidal pools, where macro algae accumulate (*Monostroma obscurum*, *Enteromorpha* sp.).

2.3. Water sampling

Table 1 summarises the sampling strategy. Monthly averaged nutrient concentrations at high tide (HT) were measured biweekly in a main channel of the lagoon (Teychan channel, Fig. 1) located close to the study site, from December 2002 to January 2004. From March 2005 to September 2006, water samples were collected bimonthly in the estuarine channel along the salinity gradient and in the major tidal creek web (Fig. 2). The tidal creek web located at north of the estuarine channel was sampled at several points. A minor tidal creek, at south of the estuarine channel, was also sampled at its mouth (Fig. 2). Sampling was performed 1h after slack tide, during ebb tide. Days of sampling were chosen when the low tide (LT) was about at twelve noon. Water samples were also collected in a tidal creek downstream the study site during whole tide cycles at the occasion of a previous investigation in year 1992-1993 (Fig. 1). Sampling was performed at spring tide, when low tide drainage was maximal. Water samples were collected every 15-30 min, from HT + 3h to LT + 1h in winter, spring, summer and fall periods (Auby et al., 1994). During spring collection, the sampling was extended to the nocturnal low tide. Water samples were collected using a 50 ml syringe and were immediately filtered through a 0.2 µm cellulose acetate syringe-filter, and kept at 4°C for nutrient analysis. Nutrient analyses (N, P and Si dissolved species) were performed back in the laboratory, the same day. An aliquot was acidified (HNO_3) for dissolved metal analysis. Salinity, pH, O_2 saturation, and water temperature were measured during the different sample collections.

2.4. Sediment sample processing

In May 2005, July 2005 and February 2006, we collected at low tide two 20 cm long cores at the level of red sand zone: one in sandy bed of the creek, the other on the mud flat, on edge of the creek (Fig. 2 & Table 1). Sub-samples were taken with 1 cm resolution from surface to 10 cm, and with 2 cm resolution for the rest of the core. For each level, another sub-sample was immediately sealed in a preweighed vial and frozen under inert atmosphere for further analyses of solid fraction and water content determination. Pore-waters were extracted by centrifuge at 4000 rpm for 20 min under inert N_2-atmosphere. For impermeable sediments, the supernatant was immediately filtered (0.2 µm cellulose acetate syringe-filter). For sandy sediments, we used centrifuge 0.2 µm filter-vials. An aliquot of filtered interstitial waters was acidified with HNO_3 for dissolved Fe and Mn analysis. A second aliquot was frozen at -25°C for nutrient analysis. The possibility that traces of oxygen have affected concentrations of reduced elements during slicing and filtration can not be excluded.

2.5. Laboratory analysis

Dissolved nitrate ($\Sigma NO_3^- = NO_3^- + NO_2^-$), ammonia and ΣCO_2 were analysed by Flow Injection Analysis (FIA) according to standard methods (Anderson, 1979; Hall and Aller, 1992). Precisions are ± 10% for ΣNO_3^- and ± 5% for NH_4^+ and ΣCO_2. Dissolved silicate, phosphate (DIP), and iron were measured by colorimetric procedures (Mullin and Riley, 1955; Murphy and Riley, 1962; Stookey, 1970; Strickland and Parsons, 1972). The precision for these methods are ± 5%. Dissolved silicate concentrations of sediment pore-waters, but not surface waters, may have been affected by the conditioning of samples by deep-freezing before analyses. Sulphate was analysed according to a nephelometric method adapted from Rodier (1976) with a precision of about 5%. Dissolved manganese was measured by flame atomic adsorption spectrometry (Perkin Elmer AA 300) with ± 5% precision. Additional data of water flow for the major river of Arcachon Bay watershed were provided by the Direction Régionale de l'Environnement-Service de la Gironde (DIREN).

Sediment was freeze-dried and the weight loss was used to calculate water content. The dried solid was homogenized for solid-phase analysis. An ascorbate reagent was used to remove from the sediment the most reactive Fe (III) phases (Fe_{asc}), all Mn (III,IV) oxides and oxihydroxides (Mn_{asc}), and associated phosphorus (P_{asc}) (Kostka and Luther, 1994; Anschutz et al., 1998; Deborde et al., 2007). A separate extraction was carried out with 1M HCl to determine acid-soluble Mn and Fe (Fe_{HCl}, Mn_{HCl}). This reagent was used to dissolve amorphous and crystalline Fe and Mn oxides, carbonates, hydrous aluminium silicates, and associated phosphorus (P_{HCl}) (Kostka and Luther, 1994). The precision estimated from replicates was ± 5% for Mn and P, and ± 7% for Fe. Particulate organic carbon (C_{org}), total carbon (C_{tot}), and total sulphur (S_{tot}) were measured on freeze-dried samples by infrared spectroscopy using a LECO C-S 125. Particulate organic carbon was measured after removal of carbonates with 2M HCl during 24 h from 50 mg of powdered sample. Inorganic carbon is the difference between total carbon and particulate organic carbon. The precision of these analyses was ± 0.02 wt%.

3. Results

3.1. Nutrient concentrations of high tide water

Averaged nutrient concentrations, measured at high tide in an adjacent main channel (Teychan), ranged from 0.2 to 26 µM (mean: 7 µM) for NO_3^-, from 0.5 to 3.5 µM (mean: 1.8 µM) for NH_4^+, and from 0.2 to 0.4 µM (mean: 0.2 µM) for DIP (Fig. 3). Maximum concentrations of nitrogen species were measured in winter and decreased during productive period, while DIP concentrations did not show significant seasonal trends.

3.2. Geochemical composition of tidal creek waters

Oxygen saturation, pH and concentrations of studied dissolved species, measured during ebb tide in estuarine and tidal creek waters, are represented versus salinity in Figure 4. For each sampling, creek waters were usually warmer and saltier probably because of shallower depth than estuarine channel, no connection with a river, and higher influence of evaporation processes (Table 2). These characteristics were naturally more pronounced in summer. In summer, the temperature of creek waters reached 32°C, whereas river water was at about 17°C. Concentrations of dissolved oxygen were lower in creek waters. Nitrate and sulphate concentrations were aligned on a dilution line in estuarine waters, whereas waters from tidal creeks were generally depleted in sulphate and nitrate relative to a mixing line (Figure 4). The mean ΣNO_3^- concentration of tidal creek was 1.8 µM, and the concentration never exceeded 6 µM. At each season, creek waters which drain the tidal flat also were characterized by a high enrichment in reduced solutes and ΣCO_2 (see Appendix A). Average ΣCO_2 and NH_4^+ concentrations were respectively up to eight and four times higher than in the estuarine channel. Maximum NH_4^+ concentrations were observed in March 2005, reaching 300 µM and 50 µM in the tidal creeks and estuarine channel, respectively. The mean NH_4^+ concentration was about 100 µM in tidal creeks. Same tendencies were noted for dissolved iron, manganese and DIP, with average concentrations twice, three times, and four times higher in creek waters, respectively. The averaged DIP concentration was 1.6 µM, and the highest concentrations reached 7 µM. Dissolved siliceous concentrations did not show clear differences between both creek systems. Waters from tidal pools sampled in upper parts of the tidal flat were characterized by a very high O_2 saturation (ranges: 180 and 305%), associated with a pH values higher than 8 (Table 1). They were generally depleted in nutrients and reduced dissolved compounds during the daytime period.

3.3. Variations of creek water geochemistry during tide cycles

In Arcachon bay, ΣNO_3^- are principally supplied by rivers, and concentrations increase with freshwater discharge (Rimmelin et al. 1998; De Wit et al., 2005). Thus, ΣNO_3^- concentrations were maximal in tidal creek during wet periods (fall and winter, Fig. 5). On a tide cycle scale, increase of ΣNO_3^- in fall corresponded to decrease of salinity, i.e. dilution with river waters during ebb. NH_4^+ and DIP concentrations always gradually increased in creek water during end of ebb to reach a maximum at low tide. Values were higher during nocturnal ebb (Fig. 6). This increase of concentration was independent of salinity. Measurements of dissolved iron and manganese concentrations were below detection limit (data not shown).

3.4. Diagenetic profiles in sediment cores

Dissolved and particulate species profiles measured on sediment cores collected on muddy edge of the creek and in the red sand zone of the creek bed are shown in Fig. 7a and 7b, respectively. The creek edge cores were characterized by a decimetre thick mud layer (mean grain size: 15 to 40 µm), which covered a permeable sandy sediment layer (mean grain size: 270 µm) (Fig.7a). The mud layer was black. We noted a strong smell of sulphide during sampling and core processing. Previous studies (De Wit et al., 2001), and our own unpublished data showed that the oxic layer was limited to the upper 1 or 2 mm on the Arcachon Bay mud flat. Salinity and sulphate concentrations in muddy and sandy layers showed a decreasing gradient from the surface to the bottom core for the sampling times. Salinity decrease was less marked in summer. In muddy sediments, early diagenesis recycled products, such as ΣCO_2, NH_4^+, DIP, dissolved iron and manganese increase directly below the surface. ΣCO_2 and NH_4^+ concentrations exceeded 3 mM and 200 µM below 2 cm depth, respectively, and gradually increased below. DIP, dissolved iron and manganese showed high concentrations in muddy layer, in comparison to underlying sands, where concentrations never exceeded 3 µM, 5 µM and 1 µM, respectively. Nitrate concentrations were lower than 5 µM in the muddy anoxic sediment. Profiles of P_{asc}, P_{HCl}, Fe_{asc}, and Fe_{HCl} showed the same pattern, with maxima in muddy layer of about 12, 22, 240 and 500 µmol g^{-1}, respectively. In sands, they decreased to reach values close to 0.5, 2, 10, 20 µmol g^{-1}, respectively. The mud layer generally presented high contents of particulate sulphur (>1.5%) and organic carbon (>3%), which represented the major part of total particulate carbon. The core collected in January 2006 showed lower values of particulate phosphorus, iron, manganese, carbon and sulphur in the muddy layer. This change may be explained by a modification of the studied sediment. In January 2006, the mud was enriched in sandy particles, and the mean grain size was 50 µm. This observation reveals the high heterogeneity and the seasonal evolution of the surface sedimentation on tidal flat. Cores collected on the bed of the creek consisted of permeable sandy sediments with a 4 cm surface layer of red sands (Fig. 7b). This layer corresponded to the high values of Fe_{asc} and Fe_{HCl} profiles (about 25 and 50 µmol g^{-1}, respectively). Concentrations decreased rapidly below 4 cm depth to reach about 10 and 15 µmol g^{-1}, respectively. Comparable vertical distributions were observed for P_{asc} and P_{HCl}. For the three sampling times, DIP concentrations were low and nearly constant with depth, close to 1.0 µM. Dissolved iron also was constant with depth, around 6.0 µM, and higher than measured in surface waters (3.2 µM). In January 2006, dissolved iron concentration drastically increased from 33 µM in surface water to about 670 µM two cm below sediment-water interface. Profiles of Mn^{2+}, Mn_{ASC} and Mn_{HCl} remained constant at values close to zero, except for the July 2005 core, where dissolved manganese increased with depth below the red sand layer. Sandy sediments C_{org}, C_{tot}, and S_{tot} contents were in the range of 0.1-0.2%. Concentrations of nitrate were generally higher just below sediment water interface than in overlying creek water. At depth, nitrate concentrations decreased. Ammonia increased rapidly in the red sand layer, and then it remained constant close to 160 µM, which was higher than surface water concentrations. We also measured a decreasing gradient of salinity and sulphate in winter and spring.

4. Discussion

4.1. Sedimentology and consequences on pore-water seeping

Sedimentology of the study site strongly influences water fluxes across sediment-water interface during low tide. During immersion, permeable sediments of upper parts of the intertidal zone (Fig. 2) become saturated with seawater by infiltration. Permeability of sand makes possible advective pore-water transport. At low tide, when pore-water table in upper sandy beach decreases, sands become unsaturated with water in the upper centimetres below the sediment surface. We observed in sands of studied cores that dilution of pore-waters with desalted waters increased during wet seasons. Therefore, underlying sands were probably affected by underground freshwater discharges, suggesting existence of a subterranean estuary more or less efficient, depending both on tide situation and season, as observed on other tidal beaches (Huettel et al., 1998; Huettel and Rusch, 2000; Charette et al., 2005). Underlying sands outcrop in the bed of studied channels. During ebb, i.e. during our sampling time, as pore-water table level drops slower than seawater level, a hydraulic gradient occurs (Nielsen, 1990). This pressure gradient causes an advective flux of pore-waters from upper sandy parts to lower parts of the flat below muddy layer. The intensity of this flux depends on hypsometric gradient. Finally, pore-waters can feed the tidal creek web at resurgence zones. Future studies on this site with geochemical tracers would enable us to estimate by modelling mean water residence time during this underground run.

Downstream, where the flat consists of impermeable muddy sediments overlaying permeable sandy sediments, we noticed important bioturbation activity driven by numerous burrows of annelida, bivalves, gasteropodan, and crabs (Blanchet et al., 2004; Blanchet et al., 2005; Cottet et al., 2007). In this area, density of annelids and bivalves burrows exceeds more than 20 000 ind m^{-2} (Blanchet et al., 2004). Consequently, profiles of reactive particulate and aqueous species in muddy sediments are controlled by early diagenetic reaction and transport by molecular diffusion, but also by advective bioturbation (Berner and Westrich, 1985; Wang and Van Cappellen, 1996). Due to cohesive nature of sediment and its low permeability, the mud remains saturated with seawater at low tide. During emersion, the tidal flat is exposed to atmosphere for several hours, and we observed that burrows became ideal ducts for pore-water seeping. Our sampling of water at low tide took place always around noon time. Uncovered mud flat was exposed to light before sampling, and it was thus heated. Consequently, most of the year, temperature of exposed mud flat was higher at low tide, in contact with atmosphere, than at high tide in contact with usually cooler flood water (data not shown). Except in winter, the temperature we measured in sampled creeks was higher than the temperature of water at high tide. Salinity of creek waters also was higher than salinity measured down core, in sandy sediments. The salinity was close to what we measured in the upper part of muddy sediments. Temperature and salinity suggest that evaporation occurs at each low tide and that the slow drainage of remaining standing water on surface mud flat is an important source of water for tidal creeks. Therefore, tidal creek waters are the sum of slow run off of standing water, pore-water seeping from muddy sediments, and to a lesser extent, seeping through permeable sediments.

4.2. The tidal pump

Surface water chemistry shows that there are two hydrous systems with distinct physical and chemical properties at low tide. The main channel is fed by a river and consequently acts as a small scale estuary. The river represents a well oxygenated source of nitrate for the system. Nitrate and sulphate concentrations are aligned on a classical mixing line relative to salinity. On the contrary, the creek waters are under-saturated in oxygen, enriched in reduced and recycled solutes, and globally depleted in sulphate and nitrate relative to a mixing line vs. salinity at low tide (Fig. 4). Creek waters are obviously different from waters collected at high tide (Fig. 3).

Sediment cores were collected without replicates (n = 1, for each season), and thus could not be used to quantitatively estimate properties such as fluxes or stocks of chemical species. Cores are however considered to be representative of pore-water nature and of occurrence of early diagenetic processes because lithology of the studied zone is homogeneous. Muddy sediment core chemistry suggests that sub-oxic and anoxic processes of organic matter mineralization occur (Fig. 7a). Underlying permeable sandy sediments show as well evidences of an enrichment of inorganic nutrients. Dilution of pore waters with fresh continental groundwater (Fig. 7b) cannot explain high nutrient concentrations in sandy sediments, because salinity profiles and nutrient profiles are uncorrelated. Thus, reduced solutes and inorganic nutrients can be transferred from muddy sediments to permeable sandy sediments by molecular diffusion at the sand-mud boundary, or by burrows that cross this boundary. Additionally, organic matter mineralization can occur also within permeable sediments located on the bed of the creek. Indeed, during flood, fresh organic matter can be introduced to the sediment by advective infiltration in upper sands, as observed elsewhere (Huettel and Rusch, 2000; Rusch et al., 2000). Previous studies have also shown that during low tide, intertidal sand flats lead accumulation of metabolic products (Rocha, 1998; Kuwae et al., 2003; Billerbeck et al., 2006a; Billerbeck et al., 2006b). Thus, tidal creek waters show an enrichment in products of early diagenesis processes, especially in ammonium and phosphate. This enrichment occurs at end of ebb whatsoever the season, due to increased influence of sediment-water exchanges on channel water chemical composition (Fig. 5 and 6). Actually, at low tide, creek water consists of sediment pore-waters originating from slow muddy sediment run off, from molecular diffusion, and from advective seeping of anoxic nutrient-rich pore-waters through numerous burrows and permeable sediments, induced by tidal pumping. The small creek sampled on the south side of the estuarine channel drains only a muddy tidal flat. Sandy permeable sediment does not outcrop on the bottom of this creek. The larger tidal creek sampled on the north side drains both mud flat and sandy sediments. Chemical composition of these two creeks is similar, which suggests that muddy sediment pore-waters contribute dominantly to chemical characteristics of creek waters at low tide. Creek waters enter in estuarine waters and despite dilution, they can supply at each ebb tide the reduced species measured in the estuarine channel and in the rest of the lagoon. Similar observations were recently revealed in another tidal bay, where tidal flushing of bottom water at low tide was evidenced by high concentrations of reduced solutes, such as sulphide, Fe^{2+} and Mn^{2+} (Lewis et al., 2007).

Permeable sediments at the bottom of the creek are enriched in ascorbate extractable iron oxides (Fig. 7b). The enriched layer probably originate from (re-)oxidation of dissolved Fe(II) present in reduced pore-waters in contact with overlying oxic waters, as observed on sandy flats by Huettel et al. (1996). The advective transit of reduced groundwater to more oxygenated environment causes a partial active re-oxidation of dissolved iron, and also manganese, which explains the 4 cm red sand layer noticed at the level of the groundwater resurgence. Phosphorus extracted by the ascorbate solution shows maximum values in this layer. It is well known that iron oxides have a great efficiency for dissolved phosphate adsorption (Krom and Berner, 1980; Sundby et al., 1992; Anschutz et al., 1998). Therefore, formation of iron oxides in sandy sediments represents a trap for dissolved P that is advected from pore-waters. In the studied creek, we observe that some dissolved Fe(II) escape the sediment, which shows that the surface sediment is not a definite barrier for dissolved Fe. Large concentrations of dissolved Fe(II) were measured in pore-water during wet periods, when the discharge of fresh ground water was significant. During these periods the bottom of sandy sediment was more red-coloured than previous periods and inputs of DIP to tidal creek waters were apparently lower than during summer period (Fig. 5). Flushing of reduced pore-waters and possibly precipitation of authigenic Fe-oxides is probably enhanced in winter, inducing a higher adsorption of phosphorus.

During nocturnal tides, nutrient inputs by tidal pumping seem to be higher than during diurnal tides (Fig. 6). This is probably due to a strengthening of anoxic processes and a drop of photosynthetic activity during night. Actually, ammonium and DIP are essential nutrients for benthic primary producers, especially seagrasses. Assimilation of these nutrients under daylight and during productive periods (Touchette and Burkholder, 2000; Welsh et al. 2000) explain the relative lower values of diurnal tides.

4.3. Estimation of nutrient inputs by the tidal pump

Waters that flow at low tide in creeks are advected from sandy and muddy sediment pore-waters. A rough estimation of nutrient fluxes during each low tide triggered by this process can be calculated. During ebb, the mean discharge runoff measured at the outlet of the studied tidal creek web ranges between 0.100 – 0.120 $m^3 s^{-1}$. The surface of drained tidal flat is estimated at about 0.114 km² with satellite images. The mean time during which the mudflat is exposed to air, and during which water outflows downstream in the tidal channel corresponds to 4h per tide cycle, i.e. 8h per day. Therefore, a total of 2880 – 3450 m^3 of water enriched in recycled products is drained by creeks each day through tidal pumping. This tidal creek water showed mean concentrations of DIP, NH_4^+ and ΣNO_3^- ranging from 1.4 to 2.3, 46.1 to 200.4 and 0.5 to 6.2 µM, respectively according to season. It represents a contribution of 1.5 – 2.9 kmol yr^{-1}, 58 – 250 kmol yr^{-1}, and 0.6 – 7.8 kmol yr^{-1}, respectively. The neighbouring river which provides fresh water to the studied small estuary, supplies 0.1 to 0.3, 0.9 to 29.6 and 14.8 to 138.2 µM of DIP, NH_4^+ and ΣNO_3^-, respectively. The mean freshwater flow was evaluated at 0.120 to 0.160 $m^3 s^{-1}$ from a two year monitoring at the river mouth (M. Canton, *pers. comm.*). The river drains a surface area of 18 km². A maximum yearly flux of nutrients was estimated at 1.5 kmol yr^{-1} for DIP, 149 kmol yr^{-1} for NH_4^+, and 697 kmol yr^{-1} for ΣNO_3^-. River remains a major source of nitrate, due to land use in the catchment area, but the tidal pump on the 0.114 km² studied tidal zone contributes yearly to a DIP and an ammonia source of the same order of magnitude as the river. Therefore, the tidal flat acts as an independent major recycled nutrient source to the ecosystem through pore-water seeping and tidal flat draining. A given surface area of tidal flat supplies as much dissolved N and P as a hundred times larger river catchment area.

Our data set allows us to attempt an upscaling exercise in order to estimate the recycled nutrient flux to water column by tidal pumping mechanism for the whole Arcachon Bay. To extrapolate data from the 0.114 km² studied part of the tidal flat to the whole intertidal zone of the lagoon (115 km²) we attempt to estimate minimal values. For that, we consider a minimal time during which the tidal pumping takes place during emersion phase, and we take into account the range of average concentrations of recycled nutrient. The time during which intertidal zone is exposed to air, and during which water flows downstream in tidal channels is 4h or less per tide cycle, depending on tidal flat location. For the following calculations, we use 1h30min per tide cycle for the whole bay, i.e. 3 h d^{-1} (2 tide cycles per day). Thus, the pore-water discharge by the tidal pumping represents about 398 – 478 × 10^6 m^3 yr^{-1}. It supplies about 556 – 1100 kmol yr^{-1}, 18300 – 95800 kmol yr^{-1}, and 200 – 2900 kmol yr^{-1} of DIP, NH_4^+ and ΣNO_3^-, respectively. These values are underestimations, because the selected emersion time is a minimal value. We can compare these values with river inputs. For the whole Arcachon lagoon, freshwater inputs are dominated by rainfalls (8%), the Leyre River (73%) and small streams (18%), that represent about 1044 10^6 m^3 yr^{-1} from a 4000 km² catchment area (Auby and Labourg, 1996; Rimmelin et al., 1998). Freshwater discharges correspond to a contribution of 460 kmol yr^{-1}, 4 500 kmol yr^{-1}, and 99 000 kmol yr^{-1} for DIP, NH_4^+ and ΣNO_3^-, respectively (Fig. 8; Rimmelin et al., 1998.). Therefore, according to the above rough estimation, at least 55% of DIP and 80% of NH_4^+ could stem from tidal drainage at low tide due to the tidal pump process (Fig. 8). This mechanism contributes for 15 – 47% of recycled dissolved inorganic N into Arcachon Bay. The nutrient mass balance of the whole lagoon includes also high sediment-water exchanges during immersion (De Wit, 1999). This part of N and P balance is not examined in this study. Welsh et al. (2000) showed that the sediment of the Arcachon Bay was a net sink for N during immersion, especially because of high seagrass uptake (N and P) during productive period. Nevertheless, the release of recycled nutrients through tidal pumping is a perennial mechanism and almost constant whatsoever the season. Thus, during periods of low nutrient inputs by freshwaters in summer, this process can support a fast primary production of phytoplankton or macroalgae, such as *Enteromorpha* sp. and *Monostroma* sp.

5. Conclusion

Billerbeck et al. (2006a, b) showed that the underground drainage mechanism through permeable sediments of tidal flat was an important nutrient source to coastal waters during ebb. Actually, they explained that water infiltration supplied solutes and particles to sands during inundation, which enhanced organic matter mineralization into sediment surface layer. The authors demonstrated that the sand flat acted as a buffer system for nutrient according a filtration cycle, due to the long residence time of pore-water. In Arcachon Bay, mineralization processes are intense, because surface sediment on the intertidal flat consists mostly of muddy and organic matter-rich sediment, thereby yielding pore-water with higher recycled nutrient concentrations than pore-water derived from sands. At low tide, seeping by percolation, diffusion or bioirrigation of these pore-waters feed a large creek web in whole lagoon. The process is extremely important in controlling the nutrient levels of the lagoon, because the flux out of the creek web integrates compounds of organic matter mineralization produced over a wide area of tidal flat. According to rough estimations on one year, nutrient exports to the pelagic system by this tidal pump provide about twice and 5 times more DIP and ammonia inputs, respectively, in comparison with river freshwater fluxes. These findings suggest that tidal flats contribute to enhance the eutrophication phenomena in the lagoon, especially in the studied system, where continental N inputs are controlled by human activities (Rimmelin et al., 1998; De Wit et al., 2005),. However, although these estimations seem to be very significant, it is essential to remind that for a nutrient mass balance, differentiation between allochthonous inputs and these recycled inputs is impossible. For that reason, both inputs cannot be added together for the calculation of total available nutrient quantity in the whole lagoon. More detailed studies are necessary to evaluate the residence time of pore-water within the intertidal flat, in order to estimate the delaying time of mineralization product feedback to the ecosystem.

Acknowledgements:

The authors gratefully acknowledge Dr H. Etcheber for particulate carbon and sulphur analysis, and S. Bujan for his assistance during sampling. We thank A. Mouret and D. Poirier who help us on the study site or in laboratory. A. Carasco mostly contributed for laboratory analyses. We also acknowledge M. Canton, the DIREN and IFREMER who provided additional data, J. Kerr for help with the English version of this paper and the anonymous reviewers for scientific and critical comments that have improved this paper. We express our gratitude to the municipality of Lanton (Gironde, France). This study was supported by the French National Programme on Coastal Environment (PNEC "Chantier Littoral Atlantique") and the ANR project PROTIDAL.

References

Agosta, K., 1985. The effect of tidally induced changes in the creekbank water table on pore water chemistry. Estuarine, Coastal and Shelf Science 21, 389-400.

Anderson, L., 1979. Simultaneous spectrophotometric determination of nitrite and nitrate by flow injection analysis. Analytica Chemica Acta 110, 123-128.

Anschutz, P., Zhong, S., Sundby, B., Mucci, A. , Gobeil, C., 1998. Burial efficiency of phosphorus and the geochemistry of iron in continental margin sediments. Limnology and Oceanography 43 (1), 53-64.

Auby, I. , Labourg, P.-J., 1996. Seasonal dynamics of *Zostera noltii* hornem. In the Bay of Arcachon (France). Journal of Sea Research 35 (4), 269-277.

Auby, I., Manaud, F., Maurer, D. , Trut, G., 1994. Etude de la proliferation des algues vertes dans le Bassin d'Arcachon, IFREMER internal report, Arcachon, pp 275.

Berner, R.A. , Westrich, J.T., 1985. Bioturbation and the early diagenesis of carbon and sulfur. American Journal of Science 285 (3), 193-206.

Billerbeck, M., Werner, U., Bosselmann, K., Walpersdorf, E. , Huettel, M., 2006a. Nutrient release from an exposed intertidal sand flat. Marine Ecology Progress Series 316, 35-51.

Billerbeck, M., Werner, U., Polerecky, L., Walpersdorf, E., deBeer, D. , Huettel, M., 2006b. Surficial and deep pore water circulation governs spatials and temporal cales of nutrients recycling in intertidal sand flat sediment. Marine Ecology Progress Series 326, 61-76.

Blanchet, H., de Montaudouin, X., Chardy, P. , Bachelet, G., 2005. Structuring factors and recent changes in subtidal macrozoobenthic communities of a coastal lagoon, Arcachon Bay (France). Estuarine, Coastal and Shelf Science 64 (4), 561-576.

Blanchet, H., de Montaudouin, X., Lucas, A. , Chardy, P., 2004. Heterogeneity of macrozoobenthic assemblages within a *Zostera noltii* seagrass bed: diversity, abundance, biomass and structuring factors. Estuarine, Coastal and Shelf Science 61 (1), 111-123.

Charette, M.A., Sholkovitz, E.R. , Hansel, C.M., 2005. Trace element cycling in a subterranean estuary: Part 1. Geochemistry of the permeable sediments. Geochimica et Cosmochimica Acta 69 (8), 2095-2109.

Cottet, M., de Montaudouin, X., Blanchet, H. , Lebleu, P., 2007. *Spartina anglica* eradication experiment and in situ monitoring assess structuring strength of habitat complexity on marine macrofauna at high tidal level. Estuarine, Coastal and Shelf Science 71 (3-4), 629-640.

De Wit, R., Leibreich, J., Vernier, F., Delmas, F., Beuffe, H., Maison, P., Chossat, J.-C., Laplace-Treyture, C., Laplana, R. , Clave, V., 2005. Relationship between land-use in the agro-forestry system of les Landes, nitrogen loading to and risk of macro-algal blooming in the Bassin d'Arcachon coastal lagoon (SW France). Estuarine, Coastal and Shelf Science 62 (3), 453-465.

De Wit, R., Stal, L.J., Lomstein, B.A., Herbert, R.A., van Gemerden, H., Viaroli, P., Cecherelli, V.-U., Rodriguez-Valera, F., Bartoli, M. , Giordani, G., 2001. ROBUST: The ROle of BUffering capacities in STabilising coastal lagoon ecosystems. Continental Shelf Research 21 (18-19), 2021-2041.

De Wit, R., 1999. The Role of Buffering capacities in STabilising coastal lagoon ecosystems, E.a.C.-. ELOISE, ENV4-CT96-0218, 2 volumes, pp 560.

Deborde, J., Anschutz, P., Chaillou, G., Etcheber, H., Commarieu, M.V., Lecroart, P. , Abril, G., 2007. The dynamics of phosphorus in turbid estuarine systems: Example of the Gironde estuary (France). Limnology and Oceanography 52 (2), 862-872.

Falcao, M. , Vale, C., 1995. Tidal flushing of ammonium from intertidal sediments of Ria Formosa, Portugal. Aquatic Ecology 29 (3-4), 239-244.

Gassiat, L., 1989. Hydrodynamique et évolution sédimentaire d'un système lagune-flèche littorale: le Bassin d'Arcachon et la flèche du Cap Ferret, Thèse d'Etat, Université Bordeaux I, pp 340.

Grigg, N.J., Boudreau, B.P., Webster, I.T. , Ford, P.W., 2005. The nonlocal model of porewater irrigation: Limits to its equivalence with a cylinder diffusion model. Journal of Marine Research 63 (2), 437-455.

Hall, O.J. , Aller, R.C., 1992. Rapid, small volume, flow injection analysis for SCO_2 and NH_4^+ in marine and freshwaters. Limnology and Oceanography 37, 1113-1119.

Huettel, M. , Rusch, A., 2000. Transport and degradation of phytoplankton in permeable sediment. Limnolology and Oceanography 45 (3), 534-549.

Huettel, M., Ziebis, W. , Forster, S., 1996. Flow-induced uptake of particulate matter in permeable sediments. Limnology and Oceanography 41 (2), 309-322.

Huettel, M., Ziebis, W., Forster, S. , Luther III, G.W., 1998. Advective Transport Affecting Metal and Nutrient Distributions and Interfacial Fluxes in Permeable Sediments. Geochimica et Cosmochimica Acta 62 (4), 613-631.

Jahnke, R.A., Alexander, C.R. , Kostka, J.E., 2003. Advective pore water input of nutrients to the Satilla River Estuary, Georgia, USA. Estuarine, Coastal and Shelf Science 56 (3-4), 641-653.

Koretsky, C.M., Meile, C. , Van Cappellen, P., 2002. Quantifying bioirrigation using ecological parameters: A stochastic approach. Geochemical Transactions (3), 17-30.

Kostka, J.E. , Luther, I., George W., 1994. Partitioning and speciation of solid phase iron in saltmarsh sediments. Geochimica et Cosmochimica Acta 58 (7), 1701-1710.

Krom, M.D. , Berner, R.A., 1980. The diffusion coefficients of sulfate, ammonium, and phosphate ions in anoxic marine sediments, Long Island Sound. Limnology and Oceanography 25 (2), 327-337.

Kuwae, T., Kibe, E. , Nakamura, Y., 2003. Effect of emersion and immersion on the porewater nutrient dynamics of an intertidal sandflat in Tokyo Bay. Estuarine, Coastal and Shelf Science 57 (5-6), 929-940.

Lewis, B.L. et al., 2007. Short-term and interannual variability of redox-sensitive chemical parameters in hypoxic/anoxic bottom waters of the Chesapeake Bay. Marine Chemistry, 105(3-4), 296-308.

Meysman, F.J.R., Galaktionov, O.S., Gribsholt, B. , Middelburg, J.J., 2006. Bioirrigation in permeable sediments: Advective pore-water transport induced by burrow ventilation. Limnology and Oceanography 51 (1 I), 142-156.

Moore, W.S., 1999. The subterranean estuary: a reaction zone of ground water and sea water. Marine Chemistry 65 (1-2), 111-125.

Morin, J. , Morse, J.W., 1999. Ammonium release from resuspended sediments in the Laguna Madre estuary. Marine Chemistry 65 (1-2), 97-110.

Mortimer, R.J.G., Krom, M.D., Watson, P.G., Frickers, P.E., Davey, J.T. , Clifton, R.J., 1999. Sediment-Water Exchange of Nutrients in the Intertidal Zone of the Humber Estuary, UK. Marine Pollution Bulletin 37 (3-7), 261-279.

Mullin, J.B. , Riley, J.P., 1955. The spectrophotometric determination of silicate-silicon in natural waters with special reference to sea water. Analytica Chemica Acta 12 162-170.

Murphy, J. , Riley, J.P., 1962. A modified single solution method for determination of phosphate in natural waters. Analytica Chemica Acta 42, 31-36.

Nielsen, P., 1990. Tidal dynamics of the water table in beaches. Water Resour Res 26, 2127-2134.

Rimmelin, P., Dumon, J.-C., Maneux, E. , GonCalves, A., 1998. Study of Annual and Seasonal Dissolved Inorganic Nitrogen Inputs into the Arcachon Lagoon, Atlantic Coast (France). Estuarine, Coastal and Shelf Science 47 (5), 649-659.

Rocha, C., 1998. Rhythmic ammonium regeneration and flushing in intertidal sediments of the Sado estuary. Limnology and Oceanography 43, 823-831.

Rocha, C., CabeÃ§adas, G. , Brogueira, M.J., 1995. On the importance of sediment-water exchange processes of ammonia to primary production in shallow areas of the Sado estuary (Portugal). Aquatic Ecology V29 (3), 265-273.

Rodier, J., 1976. L'analyse de l'eau, eaux naturelles, eaux résiduaires, eau de mer,, Dunod (Ed.). Paris, pp 364.

Rusch, A., Huettel, M. , Forster, S., 2000. Particulate Organic Matter in Permeable Marine Sands--Dynamics in Time and Depth. Estuarine, Coastal and Shelf Science 51 (4), 399-414.

Sakamaki, T., Nishimura, O. , Sudo, R., 2006. Tidal time-scale variation in nutrient flux across the sediment-water interface of an estuarine tidal flat. Estuarine, Coastal and Shelf Science 67 (4), 653-663.

Simmons, J.D.H., 1992. Importance of submarine ground-water discharge (SGDW) and seawater cycling to material flux across sediment/water interfaces in marine environments. Marine Ecology Progress Series 84 173-184.

Stookey, L.L., 1970. Ferrozine-A new spectrophotometric reagent for iron. Analytica Chemica Acta 42, 779-781.

Strickland, J.D.H. , Parsons, T.R., 1972. A practical handbook of seawater analysis. Fisheries Research Board of Canada *Bulletin* 167, 1-31.

Sundby, B., Gobeil, C., Silverberg, N. , Mucci, A., 1992. The phosphorus cycle in coastal marine sediments. Limnology and Oceanography 37, 1129-1145.

Touchette, B.W. , Burkholder, J.M., 2000. Review of nitrogen and phosphorus metabolism in seagrasses. Journal of Experimental Marine Biology and Ecology 250 (1-2), 133-167.

Wang, Y. , Van Cappellen, P., 1996. A multicomponent reactive transport model of early diagenesis: Application to redox cycling in coastal marine sediments. Geochimica et Cosmochimica Acta 60 (16), 2993-3014.

Welsh, D.T., Bartoli, M., Nizzoli, D., Castaldelli, G., Riou, S.A. , Viaroli, P., 2000. Denitrification, nitrogen fixation, community primary productivity and inorganic-N and oxygen fluxes in an intertidl *Zostera noltii* meadow. Marine Ecology Progress Series 208, 65-77.

Figure captions

Figure 1: Map of Arcachon Bay (France). Location of the study site (black circle), biweekly monitoring (black triangle), and tidal cycle sampling (black square). Grey areas indicate intertidal flats.

Figure 2: Schematic representation of the studied site viewed from the continent toward the lagoon. Locations of different water samples collected in the estuarine channel (black crosses), in the major tidal creek web, and tidal pool (open dots), in the minor tidal creek (open square), and sediment core samples (black dots). The aquiclude influences the free aquifer by fresh underground water inputs, which generate a mixing zone. It forms a decreasing salinity gradient in sandy sediments. In the bed of creeks (called regionally “Estey”), a red sand zone (dotted area) is observed at the level of underground water seeping.

Figure 3: Monthly averaged nutrient concentrations (µM) of high tide water in Teychan channel from December 2002 to January 2004: $\Sigma(NO_3^-+ NO_2^-)$ (○);NH_4^+ (Δ);PO_4^{3-} (□). Error bars represent Deviation Standard (n=4 to 8).

Figure 4: Solute concentrations of water samples collected at low tide from March 2005 to September 2006 vs. salinity: pH, Fe^{2+} (+); O_2 saturation, SO_4^{2-} (□); PO_4^{3-}, NH_4^+ (×); $\Sigma(NO_3^-+ NO_2^-)$ (♦); ΣCO2 (●); H_4SiO_4, Mn^{2+} (○). The grey areas represent the tidal creek water samples. The other points refer to estuarine channel water samples. The encircled point represents the minor tidal creek sample. The dotted lines represent the dilution line for nitrate or sulfate Full data set of solute concentration values of these water samples is available in Appendix A.

Figure 5: Evolution of nutrient concentrations in the tidal creek during ebb at the four seasons; HT: High Tide; LT: Low Tide.

Figure 6: Evolution of nutrient concentrations in the tidal creek at spring during a complete tidal cycle (day-night).

Figure 7a: Vertical profiles of dissolved and particulate species of cores collected on the creek edge in May 2005, July 2005 and January 2006. The core collected in January 2006 showed a porosity and particulate carbon content different to the other cores, which was due to a higher mean grain size.

Figure 7b: Vertical profiles of dissolved and particulate species of cores collected in the bed of creek in May 2005, July 2005 and January 2006. From the surface to 4 cm depth, permeable sediments were characterized by a red color corresponding to maxima of particulate iron concentrations.

Figure 8: Schematic sediment-water exchange diagram in Arcachon Bay during ebb. Rainfall and groundwater data come from literature and personal communications. These values are given for an arithmetic mean between inputs during dry and wet period, and between those from forest wells and urban wells. Tidal pump inputs are calculated for a mean minimal tidal pumping of 1h30min per tidal cycle. Seawater concentration data come from a biweekly monitoring on surface waters (Fig. 3).

Figure 1

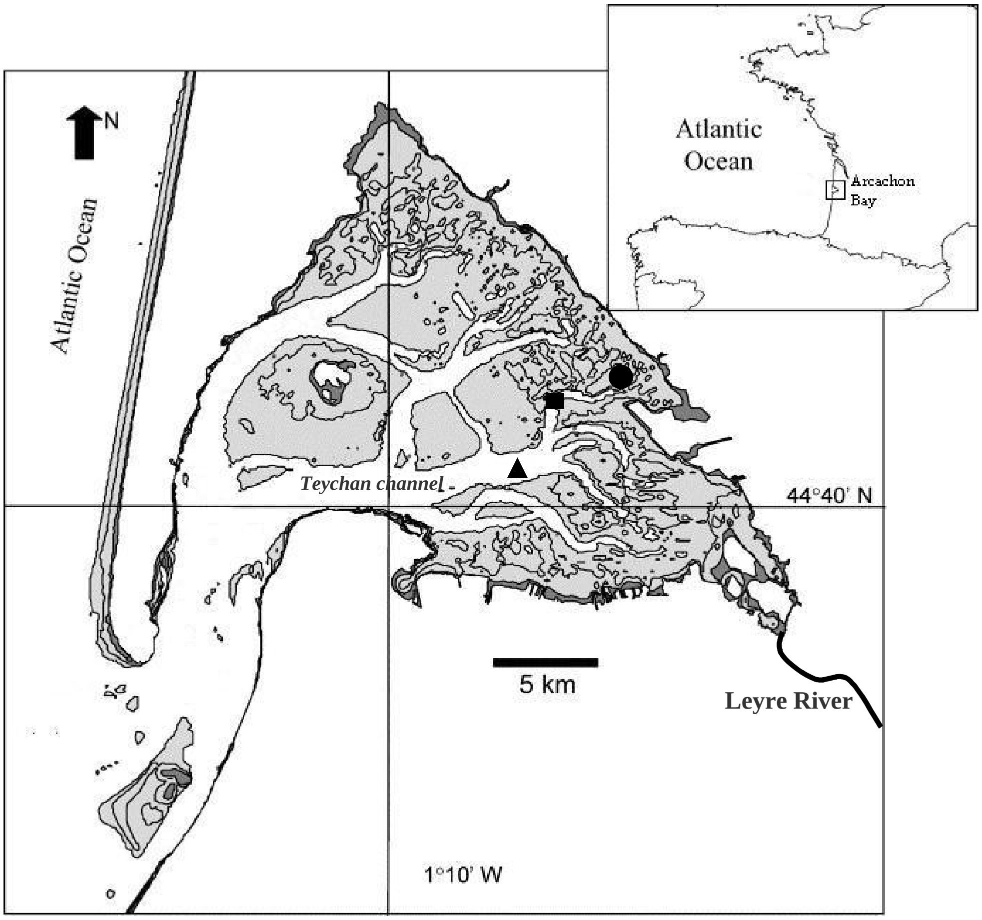

N
Atlantic Ocean
Atlantic Ocean
Arcachon Bay
Teychan channel
44°40' N
5 km
Leyre River
1°10' W

Figure 2

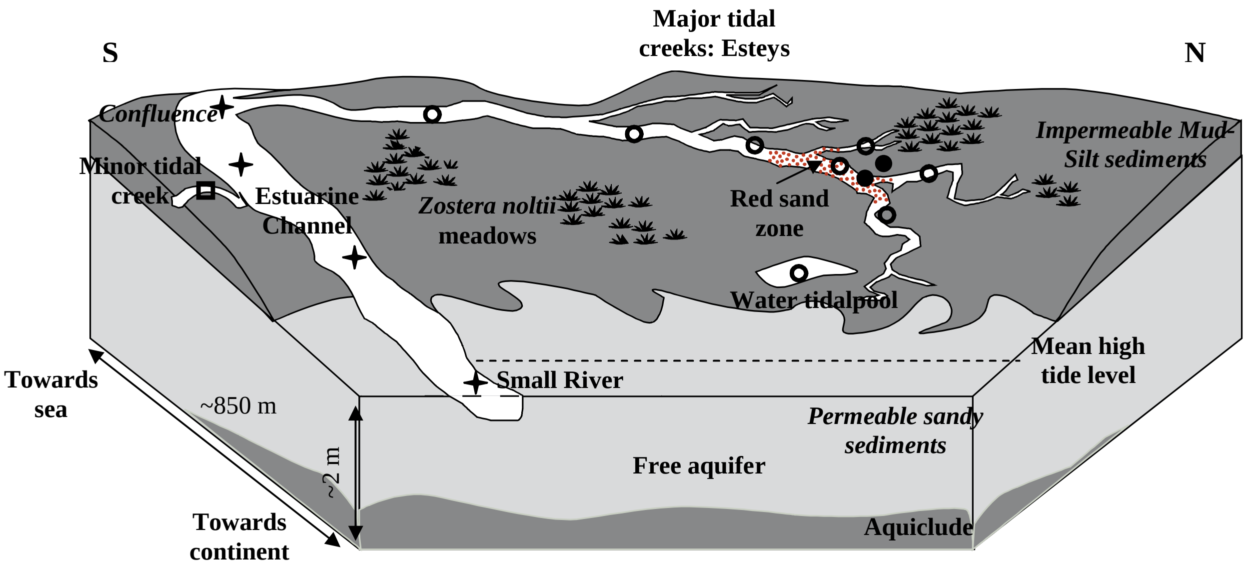

Major tidal creeks: Esteys
S
N
Confluence
Minor tidal creek
Estuarine Channel
Zostera noltii meadows
Red sand zone
Impermeable Mud-Silt sediments
Water tidalpool
Mean high tide level
Small River
Towards sea
~850 m
~2 m
Permeable sandy sediments
Free aquifer
Aquiclude
Towards continent

Figure 3

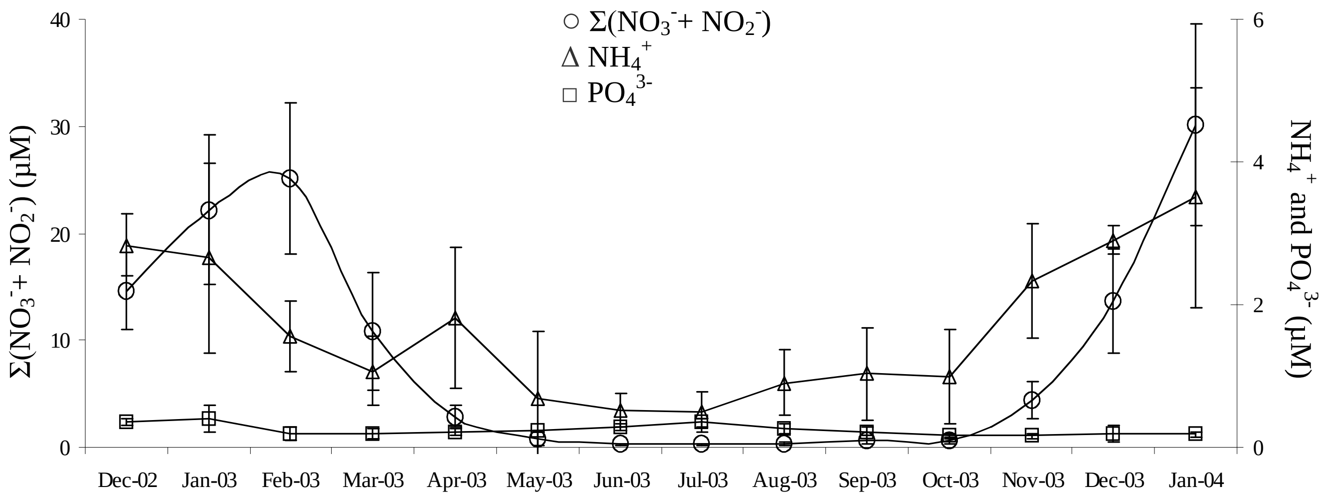

○ Σ(NO3- + NO2-)
Δ NH4+
□ PO43-
Σ(NO3- + NO2-) (μM)
NH4+ and PO43- (μM)
40
30
20
10
0
6
4
2
0
Dec-02
Jan-03
Feb-03
Mar-03
Apr-03
May-03
Jun-03
Jul-03
Aug-03
Sep-03
Oct-03
Nov-03
Dec-03
Jan-04

Figure 4

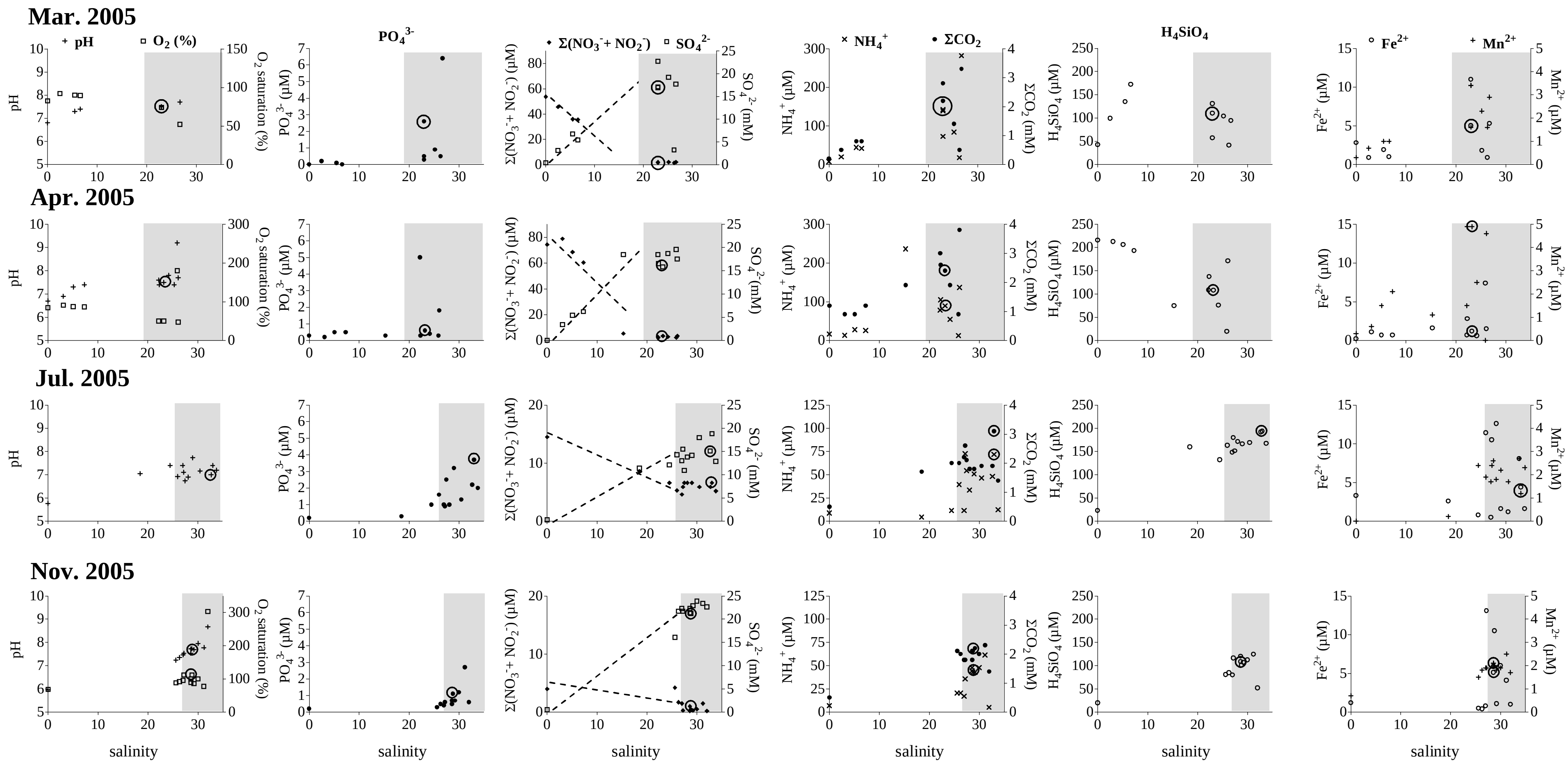

Mar. 2005
Apr. 2005
Jul. 2005
Nov. 2005
pH
O2 (%)
O2 saturation (%)
PO4 3-
PO4 3- (μM)
Σ(NO3- + NO2-)
SO4 2-
Σ(NO3- + NO2-) (μM)
SO4 2- (mM)
NH4+
ΣCO2
NH4+ (μM)
ΣCO2 (mM)
H4SiO4
H4SiO4 (μM)
Fe2+
Mn2+
Fe2+ (μM)
Mn2+ (μM)
salinity

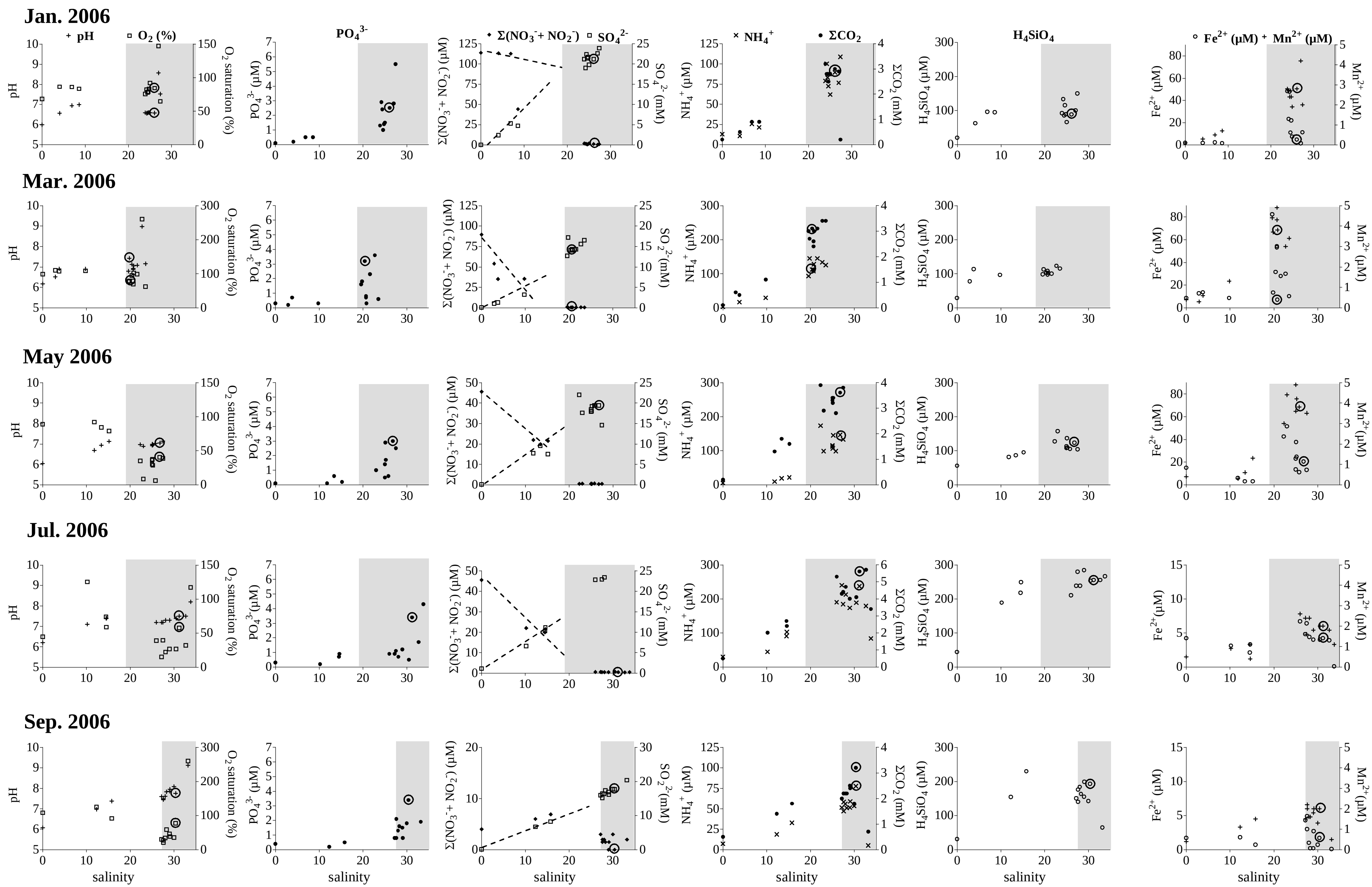

Jan. 2006
Mar. 2006
May 2006
Jul. 2006
Sep. 2006
pH
O2 (%)
O2 saturation (%)
PO4 3-
PO4 3- (μM)
Σ(NO3- + NO2-)
SO4 2-
Σ(NO3- + NO2-) (μM)
SO4 2- (mM)
NH4+
ΣCO2
NH4+ (μM)
ΣCO2 (mM)
H4SiO4
H4SiO4 (μM)
Fe2+ (μM)
Mn2+ (μM)
salinity

Figure 5

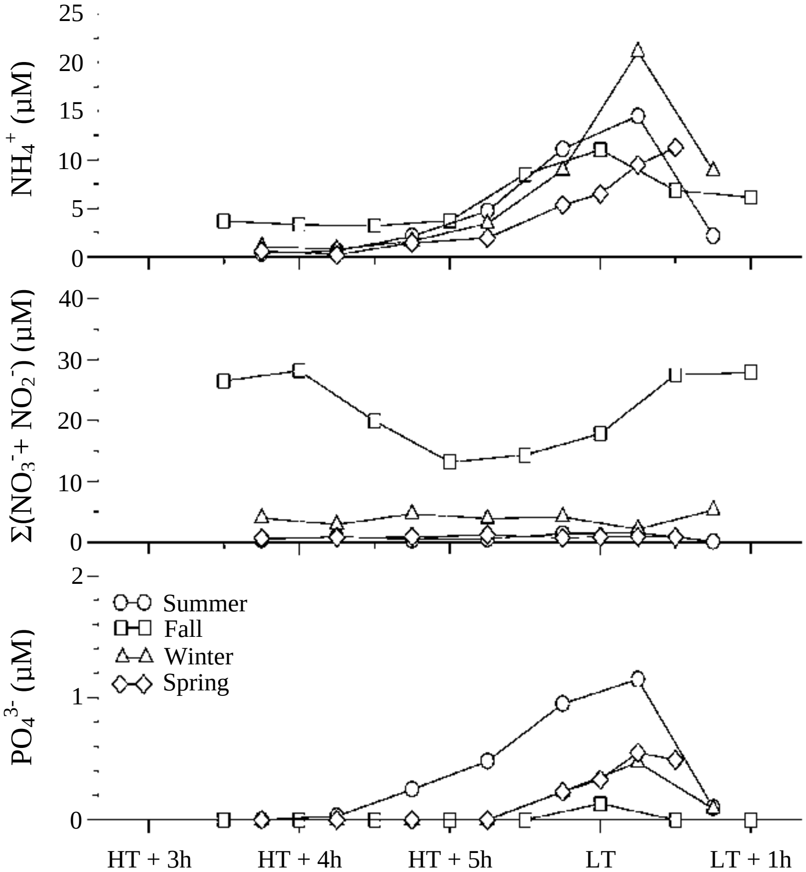

25
20
15
10
5
0
NH_4^+ (µM)
40
30
20
10
0
$\Sigma(NO_3^- + NO_2^-)$ (µM)
2
1
0
PO_4^{3-} (µM)
Summer
Fall
Winter
Spring
HT + 3h
HT + 4h
HT + 5h
LT
LT + 1h

Figure 6

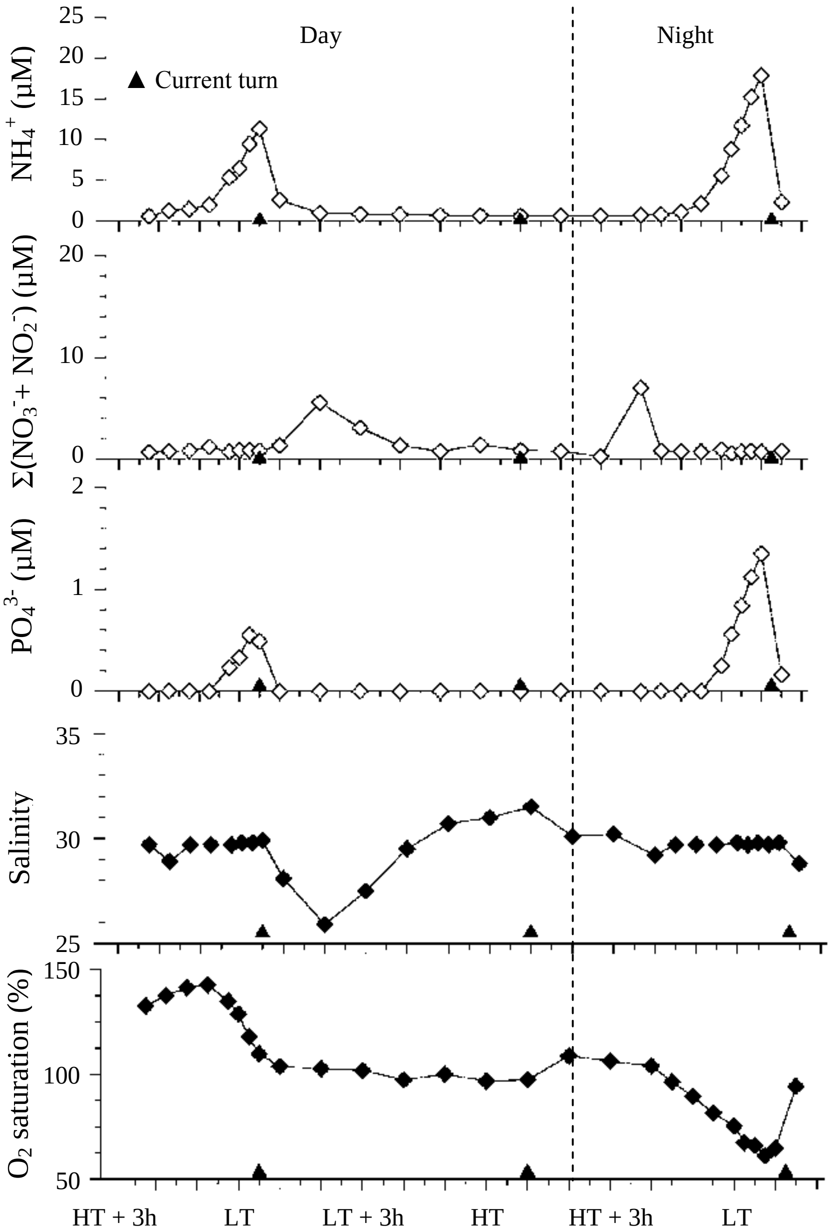
Day
Night
Current turn
NH4+ (µM)
Σ(NO3- + NO2-) (µM)
PO43- (µM)
Salinity
O2 saturation (%)
25
20
15
10
5
0
20
10
0
2
1
0
35
30
25
150
100
50
HT + 3h
LT
LT + 3h
HT
HT + 3h
LT

Figure 7a

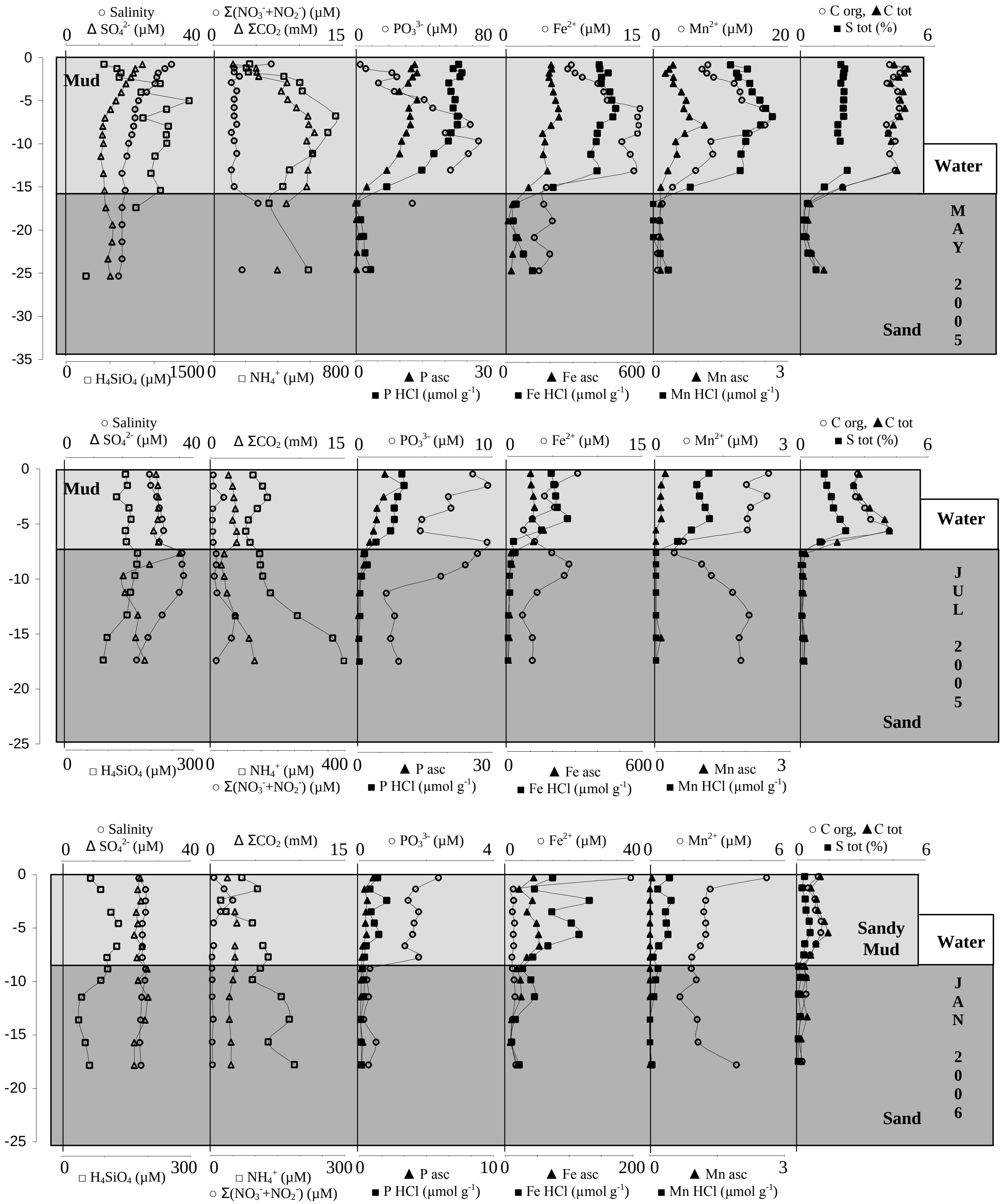

○ Salinity
Δ SO4 2- (μM)
○ Σ(NO3 -+NO2 -) (μM)
Δ ΣCO2 (mM)
○ PO4 3- (μM)
○ Fe2+ (μM)
○ Mn2+ (μM)
○ C org, ▲C tot
■ S tot (%)
Mud
Water
Sand
M A Y 2 0 0 5
□ H4SiO4 (μM)
□ NH4 + (μM)
▲ P asc
■ P HCl (μmol g-1)
▲ Fe asc
■ Fe HCl (μmol g-1)
▲ Mn asc
■ Mn HCl (μmol g-1)
J U L 2 0 0 5
Sandy Mud
J A N 2 0 0 6

Figure 7b

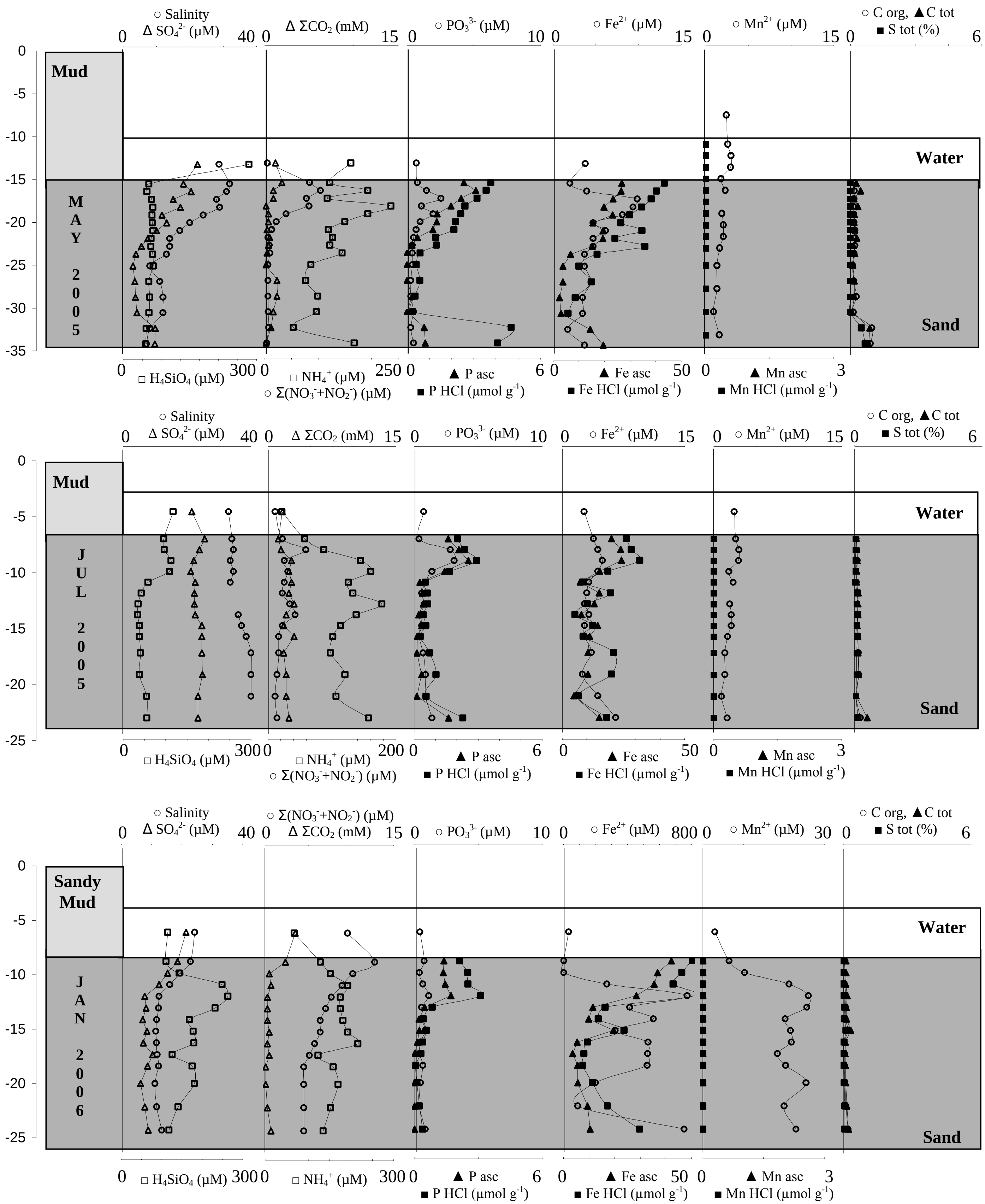

○ Salinity
Δ SO$_4^{2-}$ (µM)
Δ ΣCO$_2$ (mM)
○ PO$_3^{3-}$ (µM)
○ Fe^{2+} (µM)
○ Mn^{2+} (µM)
○ C org, ▲C tot
■ S tot (%)
Mud
Water
Sand
M A Y 2 0 0 5
□ H$_4$SiO$_4$ (µM)
□ NH$_4^+$ (µM)
○ Σ(NO$_3^-$+NO$_2^-$) (µM)
▲ P asc
■ P HCl (µmol g^{-1})
▲ Fe asc
■ Fe HCl (µmol g^{-1})
▲ Mn asc
■ Mn HCl (µmol g^{-1})
J U L 2 0 0 5
Sandy Mud
J A N 2 0 0 6

Figure 8

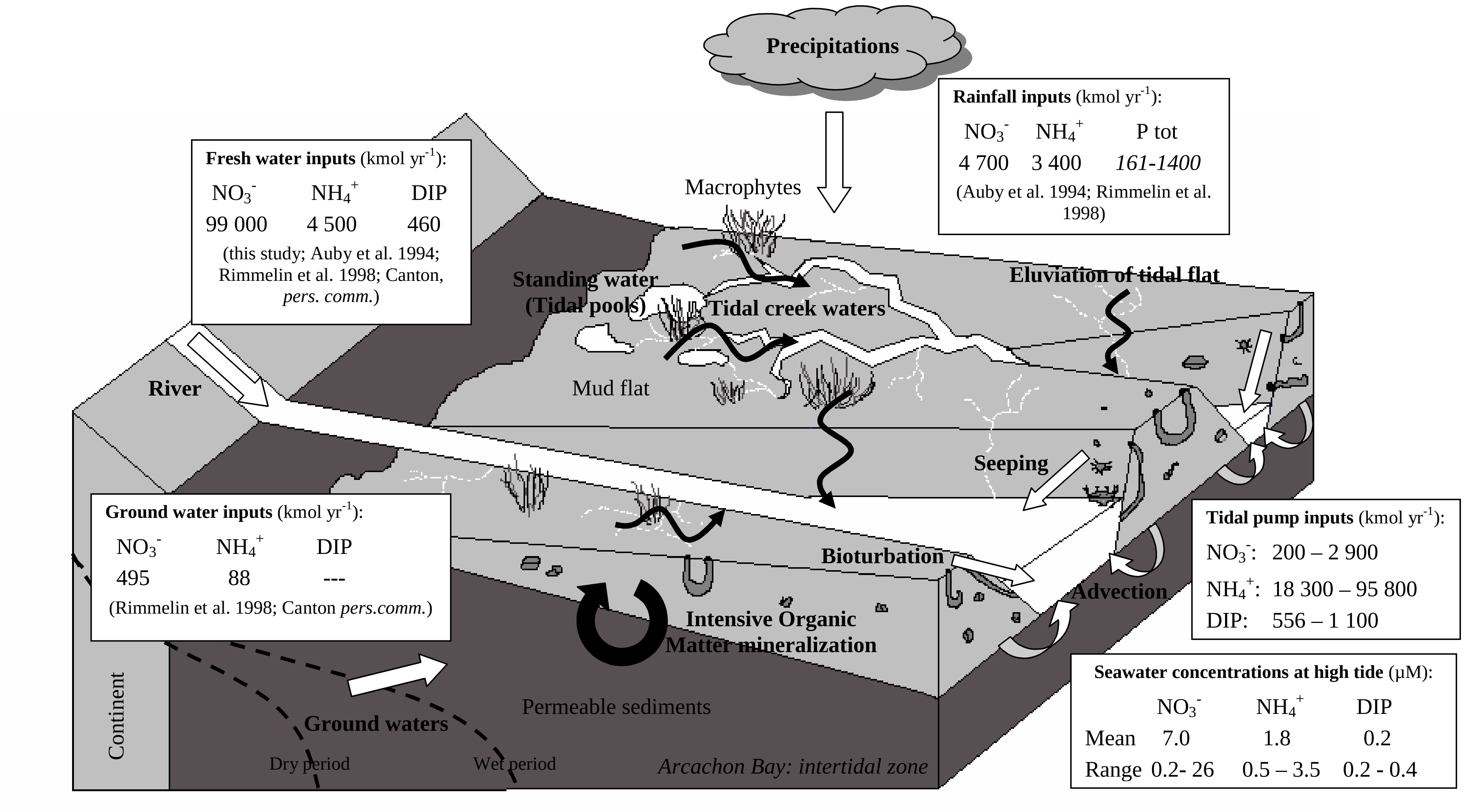

Precipitations
Rainfall inputs (kmol yr^{-1}):
NO_3^- NH_4^+ P tot
4 700 3 400 *161-1400*
(Auby et al. 1994; Rimmelin et al. 1998)
Fresh water inputs (kmol yr^{-1}):
NO_3^- NH_4^+ DIP
99 000 4 500 460
(this study; Auby et al. 1994; Rimmelin et al. 1998; Canton, *pers. comm.*)
Macrophytes
Standing water (Tidal pools)
Tidal creek waters
Eluviation of tidal flat
River
Mud flat
Seeping
Ground water inputs (kmol yr^{-1}):
NO_3^- NH_4^+ DIP
495 88 ---
(Rimmelin et al. 1998; Canton *pers.comm.*)
Bioturbation
Advection
Tidal pump inputs (kmol yr^{-1}):
NO_3^-: 200 – 2 900
NH_4^+: 18 300 – 95 800
DIP: 556 – 1 100
Intensive Organic Matter mineralization
Seawater concentrations at high tide (µM):
NO_3^- NH_4^+ DIP
Mean 7.0 1.8 0.2
Range 0.2- 26 0.5 – 3.5 0.2 - 0.4
Continent
Ground waters
Permeable sediments
Dry period
Wet period
Arcachon Bay: intertidal zone

Table 1

Table 1. Sampling procedures implemented during field work.

Sampling date	Sampling station	Sample	Frequency	Geochimical analysis
Summer 1992	6-h tidal cycle	Surface water	15-30 min	ΣNO_3^-, NH_4^+, PO_4^{3-}
Fall 1992	6-h tidal cycle	Surface water	15-30 min	ΣNO_3^-, NH_4^+, PO_4^{3-}
Winter 1993	6-h tidal cycle	Surface water	15-30 min	ΣNO_3^-, NH_4^+, PO_4^{3-}
Spring 1993	24-h tidal cycle	Surface water	15-30 min	ΣNO_3^-, NH_4^+, PO_4^{3-}
Dec. 2002 to Jan. 2004	Lagoon water (high tide)	Surface water	biweekly	ΣNO_3^-, NH_4^+, PO_4^{3-}
Mar. 2005 to Sep. 2006	Freshwater river	Surface water	bimonthly	ΣNO_3^-, NH_4^+, PO_4^{3-}, H_4SiO_4, SO_4^{2-}, ΣCO_2,Fe^{2+}, Mn^{2+}
Mar. 2005 to Sep. 2006	Estuarine channel (ebb)	Surface water	bimonthly	ΣNO_3^-, NH_4^+, PO_4^{3-}, H_4SiO_4, SO_4^{2-}, ΣCO_2,Fe^{2+}, Mn^{2+}
Mar. 2005 to Sep. 2006	Tidal creeks (ebb)	Surface water	bimonthly	ΣNO_3^-, NH_4^+, PO_4^{3-}, H_4SiO_4, SO_4^{2-}, ΣCO_2,Fe^{2+}, Mn^{2+}
May 2005	Tidal mudflat	Porewater & particulate fraction		ΣNO_3^-, NH_4^+, PO_4^{3-}, H_4SiO_4, SO_4^{2-}, ΣCO_2, Fe^{2+}, Mn^{2+}; Ascorbate and HCl extractable Fe, Mn and P; Corg, Ctot, Stot
July 2005	Tidal mudflat	Porewater & particulate fraction		ΣNO_3^-, NH_4^+, PO_4^{3-}, H_4SiO_4, SO_4^{2-}, ΣCO_2, Fe^{2+}, Mn^{2+}; Ascorbate and HCl extractable Fe, Mn and P; Corg, Ctot, Stot
January 2006	Tidal mudflat	Porewater & particulate fraction		ΣNO_3^-, NH_4^+, PO_4^{3-}, H_4SiO_4, SO_4^{2-}, ΣCO_2, Fe^{2+}, Mn^{2+}; Ascorbate and HCl extractable Fe, Mn and P; Corg, Ctot, Stot

Table 2

Table 2. Water sample characteristics: temperature, O_2 saturation, pH and salinity. For estuarine and major tidal creek samples, an average value is indicated with standard deviation in parentheses (n = 5 to 8).

Site and Date	T(°C)	O_2 (%)	pH	Salinity
Mar. 2005				
River	13.0	82.4	6.8	0.0
Estuarine channel	18.4 (2.2)	85.0 (5.2)	7.4 (0.6)	< 6.6
Major tidal creek	24.1 (2.3)	75.0 (9.8)	7.5 (0.1)	25.0 (1.7)
Minor tidal creek	23.1	74.0	7.5	23.0
Tidalpool	–	–	–	–
Apr. 2005				
River	15.1	84.8	6.7	0.0
Estuarine channel	20.0 (1.7)	87.0 (6.4)	7.3 (0.3)	< 7.3
Major tidal creek	25.0 (4.1)	50.0 (7.4)	7.5 (0.2)	22.2 (1.6)
Minor tidal creek	25.8	47.2	7.7	24.2
Tidalpool	25.2	180.0	9.2	25.9
Jul. 2005				
River	17.3	–	5.8	0.0
Estuarine channel	27.5 (4.4)	–	7.4 (0.2)	< 27
Major tidal creek	31.1 (2.6)	–	6.9 (0.3)	29.9 (2.6)
Minor tidal creek	30.0	–	7.4	33.0
Tidalpool	30.2	–	7.2	33.8
Nov. 2005				
River	14.6	68.0	6.0	0.0
Estuarine channel	16.8 (0.3)	91.8 (0.2)	7.3 (0.1)	< 26.5
Major tidal creek	20.0 (1.1)	100.1 (10.8)	7.8 (0.1)	29.2 (1.3)
Minor tidal creek	18.4	86.1	7.7	28.6
Tidalpool	20.2	302.6	8.7	32.0
Jan. 2006				
River	9.2	68.0	6.0	0.0
Estuarine channel	8.3 (0.2)	86.2 (4.7)	6.9 (0.2)	< 8.6
Major tidal creek	7.5 (0.2)	80.1 (7.2)	6.6 (0.2)	25.0 (1.2)
Minor tidal creek	7.8	64.4	7.5	27.4
Tidalpool	7.5	147.0	8.6	27.0
Mar. 2006				
River	13.6	107.0	6.9	0.0
Estuarine channel	17.0 (2.1)	100.0 (2.1)	7.1 (0.2)	< 23.5
Major tidal creek	24.5 (1.4)	85.0 (3.1)	7.4 (0.2)	19.8 (1.2)
Minor tidal creek	24.3	78.5	6.9	20.5
Tidalpool	25.0	260.0	8.9	22.7
May 2006				
River	12.0	89.0	6.0	0.0
Estuarine channel	20.0 (2.0)	86.0 (1.8)	7.0 (0.2)	< 15.2
Major tidal creek	28.7 (0.9)	32.0 (2.7)	7.1 (0.2)	28.5 (1.3)
Minor tidal creek	26.6	38.5	6.9	27.5
Tidalpool	31.1	–	–	22.3
Jul. 2006				
River	16.4	44.5	6.2	0.0
Estuarine channel	29.1 (2.2)	100.0 (1.9)	7.2 (0.2)	< 14.6
Major tidal creek	31.8 (0.8)	57.4 (7.9)	7.5 (0.2)	29.0 (2.3)
Minor tidal creek	32.4	32.0	7.3	31.2
Tidalpool	33.2	117.0	8.2	33.8
Sep. 2006				
River	22.3	108.0	6.1	0.0
Estuarine channel	23.7 (1.2)	97.0 (1.3)	7.5 (0.2)	< 28.3
Major tidal creek	25.5 (0.8)	32.0 (2.4)	7.8 (0.1)	28.5 (1.2)
Minor tidal creek	24.9	46.1	7.9	30.4
Tidalpool	27.3	260.0	9.1	33.2

Supplementary electronic material

Appendix A. Full data set of solute concentration values of the water samples collected at low tide from March 2005 to September 2006. This data set is an additional section of Figure 4.

Sampling date	Sample station	Salinity	PO_4^{3-} (µM)	$\Sigma(NO_2^-+NO_3^-)$ (µM)	NH_4^+ (µM)	H_4SiO_4 (µM)	SO_4^{2-} (mM)	ΣCO_2 (mM)	Fe^{2+} (µM)	Mn^{2+} (µM)
Mar. 2005										
	Estuarine channel	0.0	0.0	53.8	7.2	42.6	0.4	0.2	2.8	0.3
		2.5	0.2	45.7	19.3	99.2	3.1	0.5	0.9	0.7
		5.5	0.1	36.0	43.7	135.1	6.7	0.8	1.9	1.0
		6.6	0.0	35.7	41.5	172.1	5.4	0.8	1.0	1.0
	Tidal creeks	26.7	6.4	1.9	282.0	94.2	17.7	3.3	5.3	2.9
		23.0	0.3	1.6	138.8	130.6	16.9	2.2	5.0	3.4
		23.0	0.5	1.9	142.2	110.4	17.1	2.8	11.0	3.4
		23.0	2.6	1.5	72.3	57.2	22.7	2.2	5.0	1.6
		25.2	0.9	1.9	83.7	104.3	19.2	1.4	1.8	2.3
	Tidal pool	26.3	0.5	1.3	17.2	41.5	3.2	0.5	0.9	1.6
Apr. 2005										
	Estuarine channel	0.0	0.3	74.3	16.4	215.9	0.0	1.2	0.2	0.3
		3.1	0.2	78.8	13.3	212.8	3.4	0.9	1.1	0.6
		5.1	0.5	68.5	27.7	206.1	5.4	0.9	0.7	1.5
		7.3	0.5	60.4	25.7	193.3	6.2	1.2	0.7	2.1
	Tidal creeks	26.1	1.8	3.4	136.6	171.2	17.5	3.8	1.5	4.6
		23.2	0.6	3.4	89.3	108.2	15.8	2.4	1.2	4.9
		22.2	5.0	2.6	78.0	108.7	18.5	3.0	0.7	1.5
		22.3	0.3	2.3	104.7	137.4	16.5	2.6	2.8	4.9
		24.2	0.4	2.9	54.4	75.9	18.7	1.9	0.6	2.5
		25.3	0.3	5.4	236.1	74.5	18.5	1.9	1.6	1.1
	Tidal pool	25.9	0.3	2.3	12.3	19.0	19.6	0.9	7.4	0.0
Jul. 2005										
	Estuarine channel	0.0	0.2	14.5	8.8	23.2	0.3	0.5	3.3	0.0
		18.5	0.3	8.6	4.4	159.7	11.4	1.7	2.6	0.2
		24.5	1.0	6.6	11.4	131.7	12.1	2.0	0.8	2.4
		27.0	1.0	4.6	11.4	148.2	13.0	2.2	0.5	1.7
	Tidal creeks	33.0	3.7	6.6	71.8	193.6	18.8	3.1	4.4	1.2
		30.5	1.3	5.9	46.4	169.2	18.0	1.9	1.2	1.7
		29.0	3.2	6.6	50.8	166.5	14.2	1.8	1.6	2.2
		28.1	1.0	6.6	33.3	171.4	13.8	1.8	12.6	1.8
		32.7	2.2	5.9	48.1	192.2	15.1	1.9	8.1	2.7
		27.2	0.9	5.9	72.6	179.9	15.5	2.6	10.5	2.4
		27.5	2.5	6.6	54.3	151.4	10.9	2.1	43.0	2.6
		26.0	1.6	5.3	39.4	163.1	14.3	2.0	11.4	1.9
	Tidal pool	33.8	2.0	5.2	12.3	167.3	12.9	1.4	1.6	2.3
Nov. 2005										
	Estuarine channel	0	0.2	4.0	6.8	19.7	0.5	0.5	1.2	0.7
		25.6	0.3	4.2	20.5	80.9	16.1	2.1	0.5	1.5
		26.3	0.5	1.7	20.5	84.5	21.7	2.0	0.4	1.8
		27	0.4	1.5	17.1	79.4	22.3	1.8	0.8	1.9
	Tidal creeks	31.2	2.7	1.5	61.4	124.4	23.4	2.3	4.1	2.5
		29.2	0.7	0.3	42.7	107.2	22.9	2.2	1.1	1.8
		28.6	0.7	0.2	44.4	120.3	21.4	2.1	5.9	2.1

	30	1.2	0.5	47.8	112.6	23.9	2.0	6.0	1.9
	28.6	0.5	1.0	47.8	108.6	22.3	1.8	5.1	2.1
	27.2	0.6	0.3	35.8	116.4	21.7	1.8	13.1	1.9
	28.8	1.1	0.5	42.7	100.7	21.2	2.1	10.5	2.0
Tidal pool	32	0.6	0.2	5.1	51.8	22.6	1.4	1.0	1.7
Jan. 2006									
Estuarine channel	0	0.1	113.9	12.8	19.9	0.0	0.2	1.8	0.1
	4.1	0.2	113.3	10.6	62.5	2.4	0.5	1.7	0.3
	6.9	0.5	112.7	25.6	95.5	5.3	0.9	2.2	0.5
	8.6	0.5	44.1	21.3	94.4	4.7	0.9	1.5	0.7
Tidal creeks	27.4	5.5	0.9	108.6	149.5	23.9	0.2	11.3	2.0
	24.6	1.0	0.6	72.4	115.0	21.4	2.5	11.0	2.7
	23.9	1.3	1.8	78.8	92.0	21.2	3.2	48.1	2.8
	24.2	2.9	1.5	100.1	132.9	19.0	2.8	23.2	2.7
	26.1	2.5	1.2	89.4	88.2	21.2	3.0	4.8	2.8
	24.8	1.4	1.2	87.3	88.5	21.7	2.8	21.9	2.4
	25	1.5	1.8	61.8	65.5	19.8	2.8	7.4	1.9
	24.4	2.4	1.2	83.0	85.3	22.4	2.8	47.5	2.4
Tidal pool	27	2.8	0.3	76.7	99.7	22.6	2.9	1.4	4.2
Mar. 2006									
Estuarine channel	0.0	0.3	89.5	2.8	28.5	0.1	0.1	8.6	0.4
	2.9	0.2	54.1		77.4	1.0	0.6	12.7	0.3
	3.8	0.7	35.1	16.5	112.8	1.3	0.5	13.5	0.6
	9.8	0.3	35.4	29.0	96.0	3.2	1.1	8.6	1.3
Tidal creeks	23.5	0.6	0.6	125.5	115.1	16.5	3.4	10.1	3.4
	20.8	0.3	0.5	128.2	101.9	14.1	3.0	7.1	3.8
	19.8	1.8	0.3	144.8	112.1	17.2	2.7	13.3	3.7
	20.7	0.7	0.5	107.5	97.2	14.3	2.4	53.2	4.3
	21.6	2.3	0.5	144.8	99.8	14.3	3.1	27.8	5.2
	20.7	0.8	0.4	111.7	107.6	14.1	2.6	54.2	4.9
	20.4	3.2	0.5	111.7	101.9	14.1	3.1	31.4	5.8
	19.6	1.6	1.0	92.4	97.9	12.7	3.0	82.2	4.4
Tidal pool	22.7	3.6	0.7	133.7	122.9	15.6	3.4	29.8	3.0
May 2006									
Estuarine channel	0	0.1	45.5	5.4	55.7	0.1	0.2	14.9	0.4
	11.8	0.1	22.0	9.4	81.2	7.7	1.3	6.0	0.3
	13.4	0.6	19.9	18.8	86.1	9.5	1.8	3.0	0.6
	15.2	0.2	21.5	21.5	94.6	7.5	1.6	3.0	1.3
Tidal creeks	27.5	2.5	0.5	133.2	103.6	14.6	3.8	13.0	3.5
	25.8	0.6	0.7	98.2	104.7	19.4	2.8	11.1	3.8
	25	1.4	0.5	115.7	113.0	17.9	3.3	13.4	3.6
	25.2	1.7	0.5	145.3	109.2	19.2	3.4	24.5	4.2
	26.8	3.0	0.4	146.6	123.6	19.4	3.6	20.4	5.3
	25	0.5	0.6	111.7	107.6	18.4	3.4	22.9	4.9
	25.1	2.9	0.5	106.3	136.8	18.0	3.2	37.6	5.9
	23	1.0	0.6	98.2	157.4	17.6	2.9	51.4	4.4
Tidal pool	22.3	9.2	0.5	173.5	127.4	22.0	3.9	42.5	3.0
Jul. 2006									
Estuarine channel	0.0	0.3	45.5	29.6	43.7	1.1	0.5	4.2	0.5
	10.2	0.2	22.0	44.4	188.6	6.6	2.0	3.1	0.9
	14.5	0.7	19.9	90.1	217.5	10.3	2.7	2.1	1.1

	14.6	0.9	21.5	102.2	248.5	11.1	2.4	3.3	0.4
Tidal creeks	31.2	3.4	0.5	236.8	255.0	2.5	5.6	4.2	2.0
	30.5	0.5	0.7	188.3	252.9	25.4	4.1	4.0	2.0
	29.0	1.2	0.5	173.5	283.9	25.4	4.0	4.0	1.8
	28.1	0.7	0.5	212.5	237.7	23.4	4.7	4.4	2.4
	32.7	1.7	0.4	178.9	255.0	27.1	5.7	3.9	1.8
	27.2	0.9	0.6	239.4	237.7	25.7	4.3	4.8	2.4
	27.5	1.1	0.5	184.3	279.2	22.9	4.4	6.4	1.6
	26.0	0.9	0.6	189.7	210.2	22.8	5.3	6.7	2.6
Tidal pool	33.8	4.3	0.5	83.4	265.9	28.3	3.4	0.1	1.1
Sep. 2006									
Estuarine channel	0.0	0.4	4.0	7.1	31.0	0.1	0.5	1.7	0.4
	12.3	0.2	6.0	18.6	154.7	6.7	1.4	1.8	1.1
	15.8	0.5	6.9	32.7	229.7	8.2	1.8	0.7	1.5
	28.3	1.6	1.5	50.7	163.5	17.4	2.2	0.2	1.6
Tidal creeks	30.4	3.4	0.0	77.6	192.9	17.7	3.2	1.7	2.0
	29.0	1.5	0.0	51.3	155.5	16.9	2.5	0.2	1.8
	28.0	1.3	2.0	55.8	184.1	16.4	2.2	1.0	1.6
	29.1	0.8	1.5	59.0	198.7	16.2	2.4	2.7	2.0
	30.0	1.8	3.0	53.2	142.5	17.8	1.8	0.7	1.3
	27.6	0.8	2.0	58.3	140.4	15.2	2.2	3.0	2.2
	27.2	0.8	3.0	51.3	150.5	16.0	2.0	4.3	1.5
	27.6	2.1	1.5	46.8	176.1	16.5	2.2	4.9	2.0
Tidal pool	33.2	1.9	2.0	5.1	64.6	20.4	0.7	0.1	0.5